Astron. Astrophys. 338, 923–932 (1998)

ASTRONOMY AND ASTROPHYSICS

SVS 16: The most X-ray luminous young stellar object

Thomas Preibisch[1], **Ralph Neuhäuser**[2], **and Thomas Stanke**[3]

[1] Astronomisches Institut, Universität Würzburg, Am Hubland, D-97074 Würzburg, Germany
[2] Max-Planck-Institut für Extraterrestrische Physik, D-85740 Garching, Germany
[3] Astrophysikalisches Institut Potsdam, An der Sternwarte 16, D-14482 Potsdam, Germany

Received 20 April 1998 / Accepted 27 July 1998

Abstract. We present new infrared and X-ray data on the optically invisible infrared source SVS 16 in the NGC 1333 star forming region. We show that SVS 16 is a binary with a separation of $1''$. The infrared spectrum displays photospheric atomic and CO absorption lines, and thus shows that SVS 16 is a highly obscured $(A_V \sim 26\,\mathrm{mag})$ low mass young stellar object. Our infrared data allow us to derive basic stellar parameters of SVS 16. We find that the binary system probably consists of two M-type pre-main sequence stars, which seem to be younger than a few 10^5 yrs.

Our new ROSAT PSPC data confirm the previous detection with the ROSAT HRI and show that SVS 16 has an extremely high quiescent X-ray luminosity of about 2×10^{32} erg/sec in the 0.1 – 2.4 keV band, making it the young stellar object with the brightest quiescent X-ray emission ever detected. We discuss the origin of the strong X-ray emission.

Key words: stars: pre-main sequence – stars: binaries: visual – stars: individual: SVS 16 (NGC 1333) – infrared: stars – X-rays: stars

1. Introduction

Infrared young stellar objects are generally classified by the slope of their broad-band infrared spectrum between $2\,\mu$m and $10\,\mu$m (see Lada 1987; Adams et al. 1987). Class I sources have a steeply rising spectrum in that range and are generally optically invisible. They are interpreted as extremely young objects (typical age $\lesssim 100\,000$ years) which are still deeply embedded in a dense envelope of circumstellar matter. Class II sources have already accreted and/or dispersed most of their circumstellar material, are no longer embedded in a dense envelope (cf. André & Montmerle 1994) and thus visible in the optical, but still display a near-infrared (NIR) excess caused by remnant circumstellar matter. Typical examples for class II sources are the classical T Tauri stars. Class III sources exhibit no indications of an infrared excess and thus are thought to be essentially free of circumstellar matter. Typical examples are the weak line T Tauri stars, sometimes also called "naked" T Tauri stars (e.g. Walter et al. 1988). Flat spectrum sources are thought to represent an intermediate state of evolution between class I and class II.

Since the EINSTEIN era, T Tauri stars are known to be strong X-ray sources (for a recent review see Montmerle 1996), and X-ray observations have proven to be an extremely efficient tool for discovering T Tauri stars (e.g. Walter et al. 1988; Neuhäuser et al. 1995). In the last few years, very deep ROSAT and ASCA observations of star forming regions have led to some interesting detections of deeply embedded objects, which are much younger than T Tauri stars. Since X-rays with energies above $\sim$1 keV are much less affected by extinction than optical light (e.g. Ryter 1996), X-ray observations can penetrate very high column densities ($A_V \approx 30 - 40$ mag) and provide us with a deep look into dense molecular cloud cores. Up to now, X-ray emission from 6 deeply embedded class I infrared sources in the star forming regions ρ Oph (Casanova et al. 1995, Grosso et al. 1997, Kamata et al. 1997) and R CrA (Koyama et al. 1996; Neuhäuser & Preibisch 1997) could be reliably detected. The quiescent X-ray luminosities of these objects are generally rather high, ranging from a few times 10^{30} erg/sec up to several times 10^{31} erg/sec in the $0.1 - 2.4$ keV ROSAT band, i.e. factors of 10^3 to more than 10^4 above the solar level.

In a deep ROSAT HRI study of the NGC 1333 star forming region, Preibisch (1997) could detect X-ray emission from another optically invisible infrared source, known as SVS 16 (cf. Strom et al. 1976). However, unlike the objects mentioned above, SVS 16 was not well studied and it was not even clear whether it is related to the star forming region or a background object.

2. Previous observations of SVS 16

SVS 16 is one of the optically invisible infrared sources found in the near-infrared (NIR) survey of the NGC 1333 region by Strom et al. (1976); it was detected at K (2.2 μm) and L (3.5 μm), but not at J (1.2 μm) and H (1.6 μm). Aspin et al. (1994, ASR hereafter) performed a much more sensitive JHK-survey of the region and detected SVS 16 (star No 106 in ASR) in all three NIR bands, but not in their deep R- and I-band images, giving magnitude limits of $R > 21.5$ and $I > 20.0$. Finally,

Send offprint requests to: Thomas Preibisch, (preib@astro.uni-wuerzburg.de)

Aspin & Sandell (1997) surveyed the region at $3\,\mu$m and found SVS 16 to be one of the brightest $3\,\mu$m sources in that region.

Preibisch (1997) performed a deep ROSAT X-ray observation of the NGC 1333 region and could clearly detect X-rays from SVS 16. If SVS 16 actually is a young stellar object (YSO) in the NGC 1333 dark cloud, its X-ray luminosity must exceed 10^{32} erg/sec in the $0.1-2.4$ keV ROSAT band, making it the most X-ray luminous low-mass star in terms of non-flaring quiescent emission found so far. However, before accepting such a record as real, one should carefully exclude alternative explanations. While its location in a star forming region suggest SVS 16 to be a YSO, it might also be a background object not related to the star forming region at all. For example, it might be a luminous background star, or an extragalactic object like the infrared-loud quasar IRAS 13349+2438 (cf. Beichmann et al. 1986; Brinkmann et al. 1996), which shows very similar infrared and X-ray properties as SVS 16. In order to reveal the true nature of SVS 16, we have analyzed additional data and performed further infrared and X-ray observations of SVS 16, which also provide us with information about its evolutionary status.

The NGC 1333 star forming region is part of the Perseus molecular cloud complex (e.g. Bachiller & Cernicharo, 1986). The distance to this cloud complex and to its two main sites of recent or ongoing star formation, IC 348 and NGC 1333, is still a matter of debate. Rather different distance estimates ranging from 220 pc (Cernis 1990) to 500 pc (Strom et al. 1974) can be found in the literature. Here, we assume that the distance to NGC 1333 is the same as to IC 348, and use a value of 300 pc, following the detailed argumentation of Herbig (1998) concerning the distance to IC 348.

3. Infrared imaging and photometry

3.1. HST archive data

SVS 16 lies in the field of view of an archival HST observation consisting of datasets U2LS0101T to U2LS0106T. These observations were performed on 30 August 1995 with the WFPC2 camera, using the narrow band filters F656N (Hα) and F673N (SII), and the long pass filter F850LP (bandpass $0.85-1.1\ \mu$m). Two individual 2000 sec exposures were taken in each filter. We retrieved the set of calibrated data from the archive of the Space Telescope European Coordinating Facility and analyzed them using IRAF[1]. For each filter, we combined the two individual exposures with the task CRREJ, which very effectively removed cosmic rays.

SVS 16 could not be detected in the narrow band filter images, but it is clearly visible in the F850LP image (see Fig. 1). Also, it is resolved in two components. The separation of the peaks is 10.0 pixel, corresponding to $1.0''$, or 300 AU at the distance of 300 pc. Both components appear unresolved and have a FWHM of $0.15''$ (east) and $0.14''$ (west). We determined the absolute J2000 coordinates with the PIXCOD command and found $\alpha = 3^{\rm h}\,28^{\rm m}\,59.29^{\rm s}$, $\delta = +31^\circ\,15'\,47.4''$ for SVS 16-e, and $\alpha = 3^{\rm h}\,28^{\rm m}\,59.20^{\rm s}$, $\delta = +31^\circ\,15'\,47.3''$ for SVS 16-w. This agrees very well with the infrared source position given by ASR. The X-ray source position in our HRI image (Preibisch 1997) was $\alpha = 3^{\rm h}\,28^{\rm m}\,59.37^{\rm s}$, $\delta = +31^\circ\,15'\,47.5''$, i.e. $1.0''$ away from SVS 16-e and $2.1''$ away from SVS 16-w. Since the 90% confidence radius for the X-ray positional error circle is $5''$, both components of SVS 16 are clearly within the X-ray error circle (see Fig. 1).

We performed aperture photometry for both components of SVS 16 with the IRAF task APPHOT. Using the most recent photometric calibrations for filter F850LP and WFPC chip 2, we found fluxes of F(SVS 16-e) $= (5.03 \pm 0.53) \times 10^{-19}$ erg/sec/cm^2/Å and F(SVS 16-w) $= (1.35 \pm 0.08) \times 10^{-18}$ erg/sec/cm^2/Å for the effective wavelength of $0.9\,\mu$m.

3.2. UKIRT infrared imaging and photometry

In the night of 27 August 1997, infrared images of SVS 16 were obtained for us under photometric conditions as a part of the UKIRT Service Programme. The observations were performed with IRCAM3, a cooled $1-5\,\mu$m camera with a 256×256 InSb array. The plate scale was $0.286''$ per pixel. Images of SVS 16 were taken in standard J, H, K photometric filters, a nb$L$ filter ($\lambda_c = 3.41\,\mu$m, $\Delta\lambda = 0.072\,\mu$m), and a nb$M$ filter ($\lambda_c = 4.67\,\mu$m, $\Delta\lambda = 0.25\,\mu$m). The total exposure times were 300 sec in J, 50 sec in H, 25 sec in K, 120 sec in nb$L$, and 168 sec in nb$M$. For photometric calibration, standard stars were observed immediately before or after SVS 16 at nearly equal airmass.

The data were reduced in the usual way with IRAF. The dark subtracted object images were flat-fielded using a median-filtered set of object images. Then, the individual object images were mosaiced together to produce the final images. The FWHM of the point spread function in the standard star images was $0.6''-0.8''$. As an example for our NIR images, we show our J-band image in Fig. 1. SVS 16 is resolved in all NIR bands, however, the separation of the peaks is only ~ 3 pixels and thus the point spread functions significantly overlap.

We utilized two different techniques to perform photometry for SVS 16. First, we performed PSF fitting photometry for the individual components of SVS 16, using the DAOPHOT package in IRAF, and also a PSF fitting routine in MIDAS. In both cases, we used the standard stars to compute the PSF models. Second, we performed aperture photometry for the binary system, using an aperture radius of $6''$. Such a large aperture should include possible extended emission around the binary system.

We related the nb$L$ and nb$M$ fluxes directly to the broad band L and M fluxes of the standards. The photometric results are summarized in Table 1, where we also give the magnitude differences in each band and the summed magnitudes for the binary system.

[1] IRAF is distributed by the National Optical Astronomy Observatories, which are operated by the Association of Universities for Research in Astronomy, Inc., under cooperative agreement with the National Science Foundation.

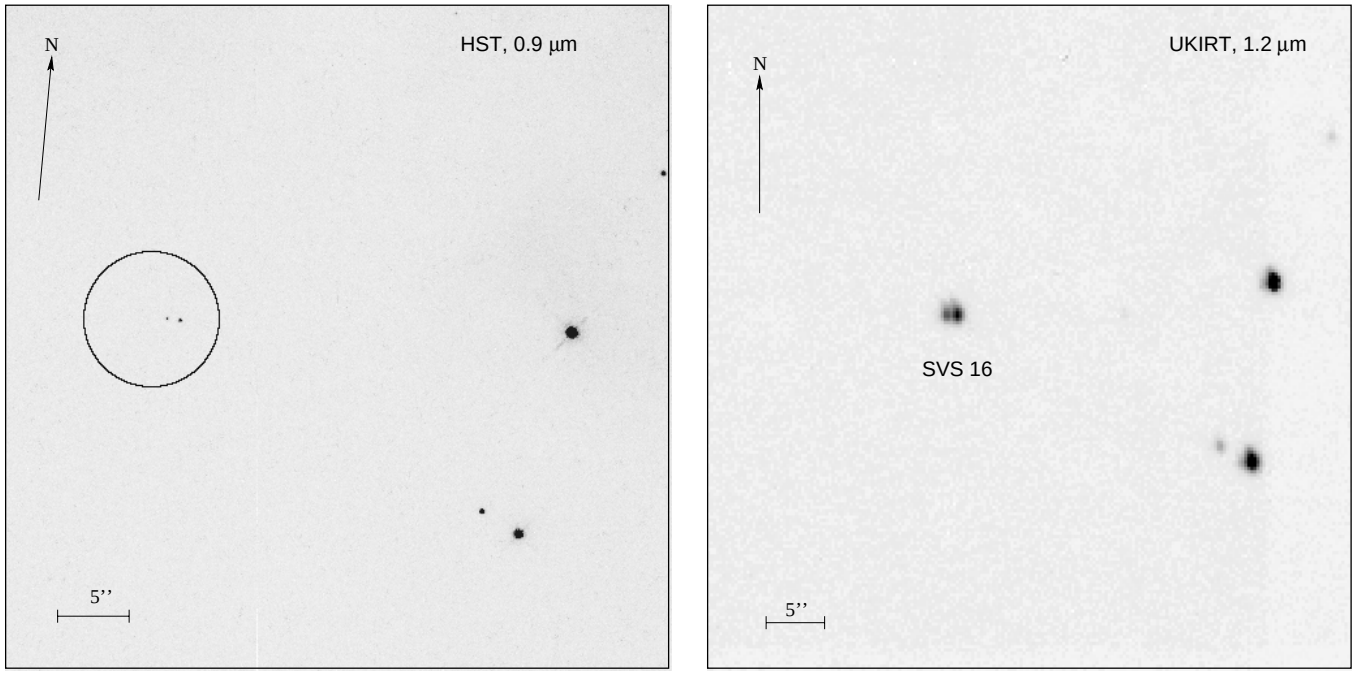

Fig. 1. Images of SVS 16: Left: HST image, taken with filter F850LP and showing a field of view of about $50'' \times 50''$. The 90% confidence error circle for the ROSAT HRI X-ray source position is shown. Right: UKIRT J-band image, showing a slightly larger field of view.

Finally, we compare our results to the J, H, K magnitudes found by ASR and the L magnitude reported by Aspin & Sandell (1997, AS hereafter). Both of these studies also used IRCAM, however with a considerably larger pixel size of $1.24''$ for ASR, and $0.62''$ for AS, and thus the SVS 16 binary system was not resolved in their data. For the J, H, K data our combined magnitudes agree very well with the ASR results. At L, our result seems to deviate significantly from the magnitude given by AS. This might be related to the use of different nb$L$ filters.

The location of SVS 16 in the NIR color-color diagram is shown in Fig. 2. Both components lie only slightly outside the reddening band and thus show a small NIR excess. A comparison with other YSOs shows that the NIR excesses of the components of SVS 16 are more similar to those of class II or class III sources rather than those of class I or flat spectrum sources.

3.3. $10\,\mu$*m imaging*

In the night of 2 December 1996 we used the ESO mid-IR camera TIMMI (Käufl et al. 1994) at the 3.6 m telescope on La Silla to obtain $10\,\mu$m images of the SVS 16 region. This camera contains a 64×64 pixel Gallium doped Silicon array, cooled with liquid Helium. Chopping of the secondary mirror and nodding of the telescope was used to subtract the strong thermal background radiation. No flatfield correction was applied to the images, since the sensitivity of the array is uniform within ∼20% . The N broad band filter ($\lambda_c = 10.1\,\mu$m, $\Delta\lambda = 5.1\,\mu$m) was used. The pixel scale was $0.5''$ per pixel, yielding a field of view of $\sim 32'' \times 32''$. The total integration time was 26 minutes. No source was detected in the image. We estimate a point source sensitivity of ∼0.25 Jy for our image and will use this value as upper limit for SVS 16.

3.4. Upper limits from other observations

3.4.1. IRAS data

We have searched the IRAS Point Source Catalogue and Faint Source Catalogue for a possible IRAS detection of SVS 16. The only potential IRAS counterpart for SVS 16 is FSC 03258+3105, which lies about $40''$ away from SVS 16. However, this FSC source is also only $40''$ away from IRAS 2, a well studied protostellar object with strong far infrared emission (cf. Sandell et al. 1994). It is much more likely that IRAS 2 rather than SVS 16 is the true counterpart of the FSC source. We thus conclude that SVS 16 was not detected by IRAS. Its position between the strong sources IRAS 2 and SVS 13 makes it very difficult to say something about the far-infrared emission from SVS 16. We thus use the fluxes for FSC 03258+3105, i.e. $F_\nu(12\,\mu\text{m}) = 13.6$ Jy, $F_\nu(25\,\mu\text{m}) = 46.5$ Jy, $F_\nu(60\,\mu\text{m}) = 204$ Jy, and $F_\nu(100\,\mu\text{m}) = 380$ Jy, as upper limits for SVS 16.

3.4.2. $350\,\mu$m flux

Recently, a $350\,\mu$m survey of the NGC 1333 star forming region was performed with SHARC, a linear array of 24 bolometers at the Caltech Submillimeter Observatory 10.2 m telescope on Mauna Kea (cf. Hunter et al. 1996). SVS 16 could not be detected in the SHARC data, to an upper flux limit (3σ) of 6.1 Jy

Table 1. HST- and UKIRT-Photometry for SVS 16 compared with literature data.

band	SVS 16-e [mag]	SVS 16-w [mag]	difference [mag]	sum [mag]	$6''$ aperture [mag]	ASR [mag]	AS [mag]
ST_{850}	24.63 ± 0.16	23.55 ± 0.08	1.07	23.21 ± 0.14			
J	17.17 ± 0.05	16.38 ± 0.05	0.80	15.95 ± 0.07	15.91 ± 0.05	15.83 ± 0.07	
H	13.56 ± 0.07	12.91 ± 0.06	0.65	12.43 ± 0.09	12.35 ± 0.03	12.50 ± 0.07	
K	11.37 ± 0.05	10.85 ± 0.05	0.52	10.33 ± 0.07	10.33 ± 0.03	10.39 ± 0.07	
L	9.55 ± 0.10	9.23 ± 0.10	0.32	8.63 ± 0.14	8.75 ± 0.11		8.36 ± 0.05
M	9.04 ± 0.13	8.65 ± 0.10	0.40	8.07 ± 0.16	7.91 ± 0.25		

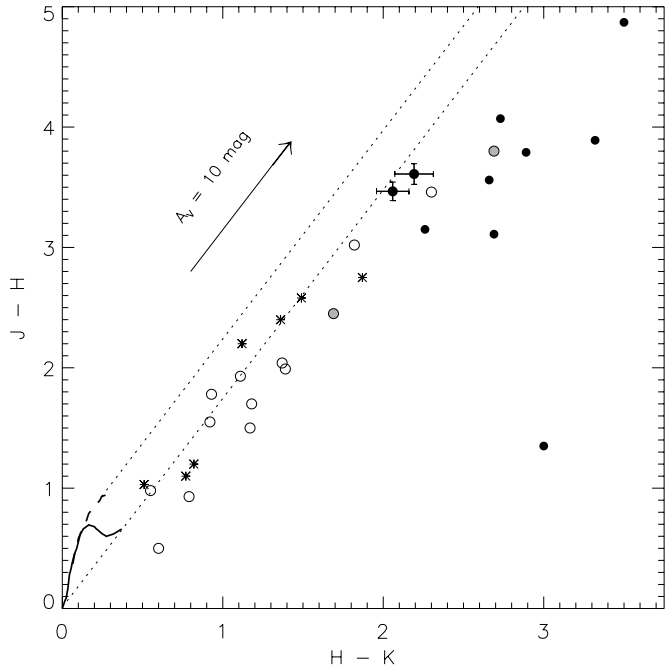

Fig. 2. NIR color-color diagram for SVS 16 and other YSOs. The solid dots with the error bars show SVS 16-e and SVS 16-w. For comparison we also have included data from Barsony et al. (1997) for those YSOs in the ρ Oph star forming region for which Greene et al. (1994) determined infrared classes. The solid dots show class I sources, grey dots flat spectrum sources, open circles class II sources, and asterisks class III sources. Furthermore, we have included 5 class I sources in the CrA core (Wilking et al. 1997). The solid line shows the main sequence, the dashed line the giant branch. The dotted lines show the reddening band for main sequence colors, the arrow shows the reddening vector for $A_V = 10$ mag.

within a $30''$ diameter aperture (M.A. Nassir and J.R. Deane, priv. comm.).

3.4.3. 1.3 mm flux

Lefloch et al. (1998) presented very sensitive 1.3 mm continuum and CS maps of the NGC 1333 cloud. No source could be found at the position of SVS 16. Due to its proximity to the bright mm source SVS 13, it is quite hard to derive an upper limit for the mm flux of SVS 16. We note that SVS 16 would have probably been detected, if its mm flux were as strong as that of the weak core Cor1, for which a flux of 57 mJy per beam was found. We will use this value as an upper limit for the 1.3 mm flux of SVS 16.

4. Infrared spectroscopy

4.1. Observations and data reduction

K- and H-band spectra of SVS 16 were obtained for us as a part of the UKIRT Service Programme. The observations were performed with CGS4, a $1 - 5\,\mu$m multi-purpose 2D grating spectrometer containing a 256×256 InSb array. In the night of 17 February 1997, K-band spectroscopy was performed with a 75 l/mm grating, in the night of 25 October 1997, a H-band spectrum was obtained using a 40 l/mm grating. SVS 16 turned out to be too faint for obtaining a usable J-band spectrum.

Since the slit width was $1.23''$, the spectra contain contributions from both binary components. In the K-band, the total exposure time for SVS 16 was 160 sec, the B8V star BD +30°540 was observed as a calibration star and an Argon lamp spectrum was used for wavelength calibration. In the H-band, the total exposure time for SVS 16 was 240 sec, the A2V star BS 1041 was observed as a calibration star and a Xenon lamp spectrum was used for wavelength calibration.

The first step of the data reduction was to remove the tilt of the spectra to the direction perpendicular to the dispersion. Then, we differenced object and sky frames, extracted the positive and negative spectra with the IRAF task APALL, and co-added all spectra. In order to remove the instrumental and atmospheric features in the spectra, we divided the object spectrum by the spectrum of the early type calibration star, from which we had removed the H I absorption lines. Finally, the resulting spectrum was multiplied by a Planck function at a blackbody temperature equal to that of the calibration star. The features and shape of the final spectra should be representative of the true object spectrum. For further details on NIR spectral data reduction we refer to Greene & Lada (1996).

The resulting spectrum is shown in Fig. 3. The effective resolution is $R \sim 750$ for the K-band spectrum and $R \sim 400$ for the H-band spectrum. The signal to noise ratio is ~ 150 in the K-band and $\sim 50 - 100$ in the H-band. Several atomic and

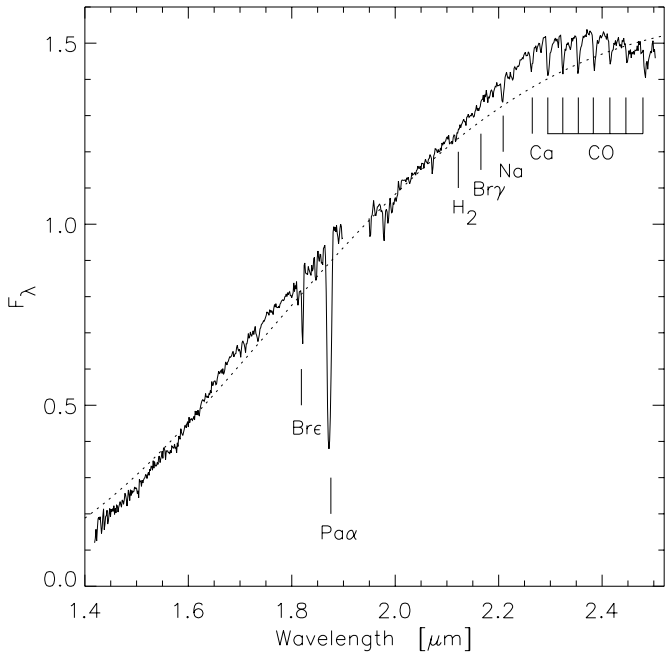

Fig. 3. This plot shows the H- and K-band spectrum of SVS 16. The positions of important lines are marked. The dotted line is a Planck function of $T = 3500$ K reddened by $A_V = 26$ mag as determined in Sect. 4.2.

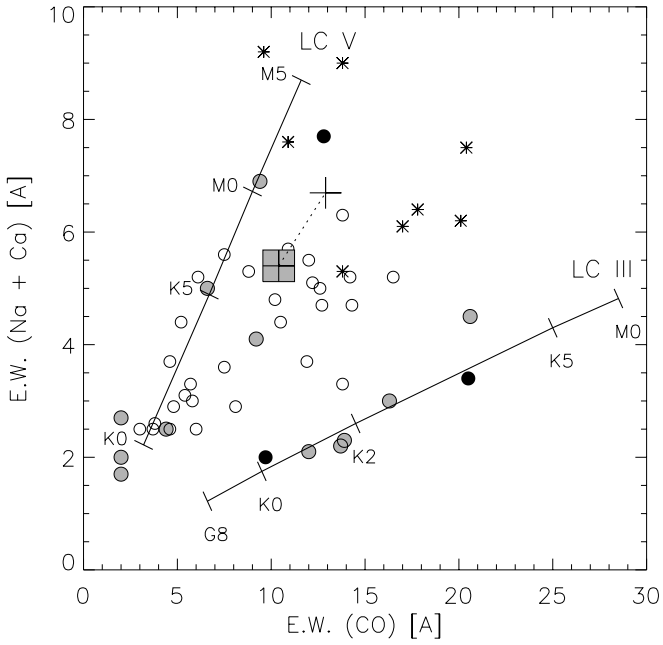

Fig. 4. Diagram of line widths, adapted from Greene & Lada (1996). The big grey rectangle shows the position for SVS 16, the size of the symbol corresponds to the errors. The cross connected to the rectangle by the dotted line indicates the position after correcting for veiling. We also have included other YSOs from Greene & Lada (1996). The assignment of infrared class to plot symbol is as in Fig. 2.

Table 2. Line widths in the K-band spectrum.

line	Na	Ca	CO [0-2]	CO [2-4]
λ [μm]	2.21	2.26	2.29	2.35
EW [Å]	3.1	2.3	4.9	5.5

CO absorption lines can be clearly seen. The most prominent lines are identified in Fig. 3. The presence of these absorption lines clearly shows that SVS 16 is a late type stellar object. The spectrum does not show any emission lines, which are found in some YSOs. Also, no line can be seen at the position of Br γ. The seemingly strong Pa α and Br ϵ absorption lines probably are artifacts caused by the strong blending of these lines with atmospheric extinction lines in the standard spectrum.

4.2. Determination of spectral types

We have used the line widths measured from the K-band spectrum and summarized in Table 2 to estimate the spectral type and surface gravity with the method presented by Greene & Meyer (1995). The location of SVS 16 in the diagram of atomic versus CO indices is shown in Fig. 4, where we also show the calibration lines from Greene & Meyer (1995) for stars of luminosity class V and III. However, one cannot directly read off the spectral type from the position in this diagram, since we have to take into account spectral continuum veiling, which is caused by the excess emission from hot circumstellar matter. In order to correct for this veiling, we used the iterative procedure described by Greene & Meyer (1995). We assumed veiling to be significant in the K-band only, what can be justified by the very modest NIR excess of SVS 16 as inferred from its position in the color-color diagram, and used the reddening relations $A_V = 9.37\ E(J-H) = 3.55\ A_J = 16.25\ E(H-K) = 8.93\ A_K$ (cf. Rieke & Lebofsky 1985). Furthermore, we assumed that the spectrum is dominated by SVS 16-w, which is nearly twice as bright as SVS 16-e in the K-band and we thus related all properties derived from the spectrum to SVS 16-w.

The uncorrected line widths suggest a spectral type ∼K7 and a veiling factor $r_k = 0.33$. Using this veiling factor to correct the line widths results in a new estimate of the spectral type, which again can be used to obtain a new veiling factor, and so on (see Greene & Meyer 1995 for details). This iteration procedure converged within 3 steps, yielding a spectral type M2, an extinction of $A_V = 26.2$ mag, and a veiling factor of $r_k = 0.24$. Finally, we computed the luminosity from the dereddened J-band magnitude, using the BC_J bolometric correction from Hartigan et al. (1994) and find $L_\star = 3.83\,L_\odot$ We note that a Planck function for a temperature corresponding to spectral type M2 and reddened by 26 mag of visual extinction reproduces the general shape of the spectrum quite well (see Fig. 3). For the uncertainties of the derived parameters we assume ± 2–3 subclasses in spectral type and ± 0.2 in $\log L_\star$.

What can we say about SVS 16-e? We know that it is fainter and redder; this might be caused by higher extinction, a later spectral type, or both. It is not possible to disentangle this with the available data. All we can do is to assume a spectral type

Table 3. Stellar parameters for SVS 16

	SVS 16-w	SVS 16-e
$L_\star$ $[L_\odot]$	3.8	2.7
SpT	M2	M3:
$R_\star$ $[R_\odot]$	5.3	4.9
A_V [mag]	26.2	28.0
r_k	0.24	0.22
age [yrs]	$\lesssim 10^5$	$\lesssim 10^5$

and then compute extinction and luminosity. However, we note that in most T Tauri binary systems the components seem to be coeval (cf. Brandner & Zinnecker 1997; Ghez et al. 1997). If we assume a spectral type of M3, we find $A_V = 28.0$ mag, a luminosity of $L_\star = 2.70\,L_\odot$, and then SVS 16-e and SVS 16-w lie roughly parallel to the isochrones in the HR diagram. Thus we prefer this set of parameters. Of course, due to this indirect argument, the uncertainties for the parameters of SVS 16-e are are higher than for SVS 16-w; we assume ± 3 subclasses in spectral type and $\Delta \log L_\star \sim \pm 0.3$.

5. The evolutionary state of SVS 16

The K-band spectrum clearly shows that SVS 16 is a late type PMS star and not an extragalactic object. The analysis of the line widths also shows that SVS 16 is more similar to a dwarf star rather than a giant. This is a clear argument against the interpretation as a giant star behind the star forming region. Further evidence for this comes from the X-ray properties (see next section): We find a (distance independent) fractional X-ray luminosity of $L_{\rm X}/L_{\rm bol} = 8 \times 10^{-3}$ for SVS 16, while late type giant stars generally show much lower ratios of $L_{\rm X}/L_{\rm bol} \lesssim 10^{-5}$ (cf. Hünsch et al. 1996). Thus we conclude that SVS 16 is not a luminous background star. Since it obviously cannot be a foreground star, it must be related to the star forming region.

5.1. Location in the HR diagram

With the available data it is possible to place SVS 16 into the HR diagram and compare its position with PMS evolutionary tracks. In Fig. 5 this is done using the tracks from D'Antona & Mazzitelli (1994). Both components of SVS 16 lie above the 10^5 yrs isochrone and the birthline. Taking into account the uncertainties of the stellar parameters and also in the theoretical tracks, we restrict ourself to the conclusion that SVS 16 is younger than a few 10^5 yrs, i.e. a very young PMS object. We note that SVS 16 has a quite similar position in the HR diagram as the very young flat spectrum source VSSG 17 (Greene & Lada 1997). A comparison with the recent tracks of Siess et al. (1997) confirms our upper limit for the age.

Even if the distance to the NGC 1333 star forming region were only 220 pc instead of the 300 pc we use here, SVS 16 would still lie significantly above the 10^6 yrs isochrone and the birthline, and none of our conclusions would be changed significantly.

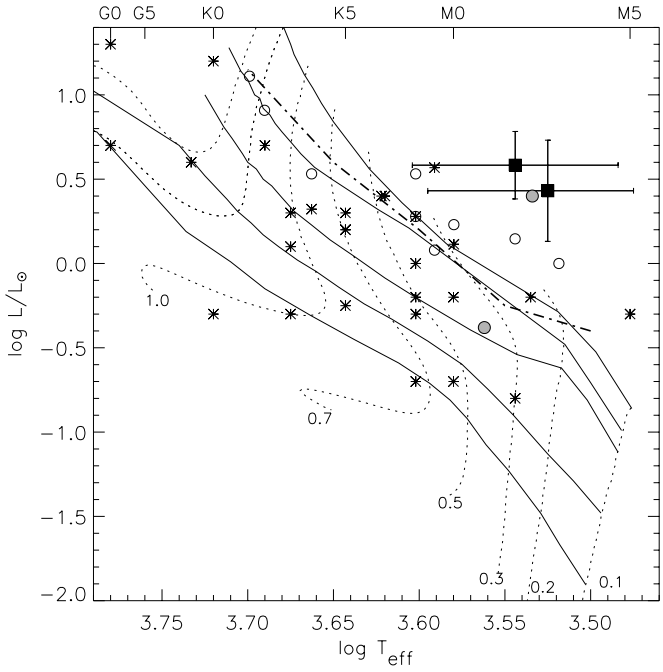

Fig. 5. HR diagram with isochrones and PMS evolutionary tracks from D'Antona & Mazzitelli (1994). The solid lines show the isochrones for ages of 0.1, 0.3, 1, 3, and 10 Myrs. The dotted lines show evolutionary tracks which are labeled by the corresponding masses in solar units. The thick dashed-dotted line shows the birthline according to Palla & Stahler (1990). The positions for both components of SVS 16 are shown by the solid squares. Other YSOs are from Greene & Meyer (1995) and Greene & Lada (1997). The assignment of infrared class to plot symbol is as in Fig. 2.

5.2. Infrared class and circumstellar environment

Since we only have upper limits to the flux beyond $5\,\mu$m, it is not possible to determine the infrared class, which is usually given by the slope of the spectrum between $2\,\mu$m and $10\,\mu$m. In Fig. 6 we show the broad-band NIR spectral energy distribution for both components of SVS 16. Although our upper limit to the $10\,\mu$m flux does formally not exclude the classification as a class I source, the spectral slope between $3.5\,\mu$m and $4.8\,\mu$m suggests SVS 16 to be a class II or class III source. A comparison with the reddened colors of stellar photospheres for the spectral parameters as found above, shows that both components exhibit small infrared excesses, which seem to peak near $3.5\,\mu$m.

Further information can be derived by comparing our spectrum of SVS 16 to those of other YSOs (cf. Greene & Lada 1996). The presence of atomic and CO absorption lines is rather untypical for class I sources, most of which display strongly veiled featureless spectra. The spectrum of SVS 16 looks more like that of class II or class III sources. Another argument can be based on the K-band veiling determined above. Our value of $r_k = 0.23$ is consistent with SVS 16 being an infrared class

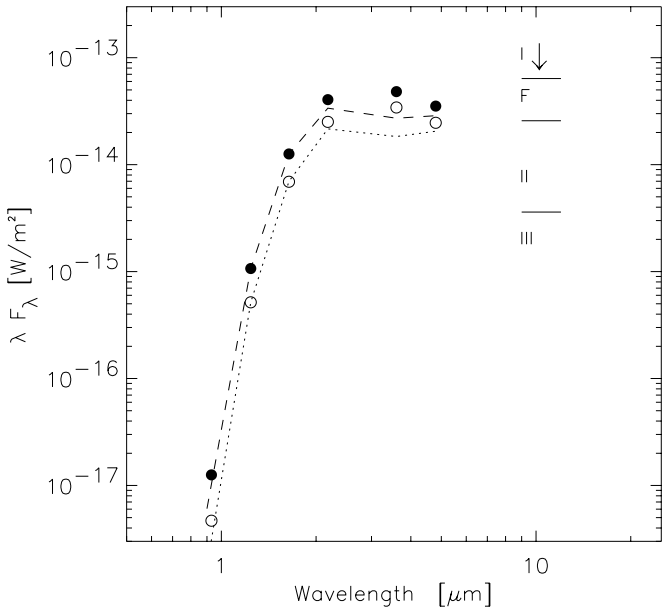

Fig. 6. Spectral energy distribution for SVS 16-e (open circles) and SVS 16-w (solid circles). The arrow marks the upper limit for the $10\,\mu$m flux. The flux limits for the different infrared classes, i.e. I, flat (F), II, and III, are indicated by the horizontal lines at $10\,\mu$m. The dashed and dotted lines show model SEDs constructed from the empiric colors of M2 and M3 stars with appropriate reddening (see Sect. 4.2) which are normalized to the J-band fluxes of SVS 16-w and SVS 16-e, respectively.

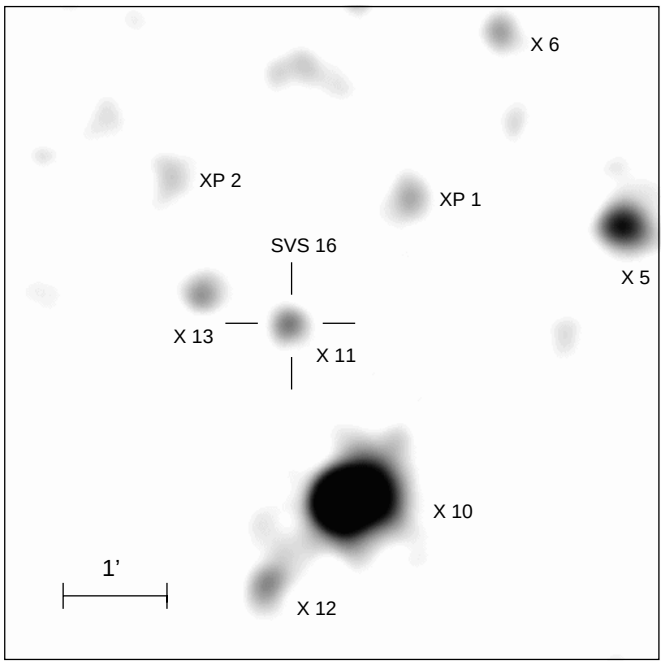

Fig. 7. Illustration of the X-ray sources in the SVS 16 region. In order to create this image, we merged the PSPC and the HRI data and finally smoothed the image with a Gaussian filter. Source numbers are indicated next to each detected X-ray source. The cross marks the HST position of SVS 16. Note that this image is only meant to be an illustration and was not used for source detection or count rate determination.

II or III object rather than a class I or flat spectrum object (see Fig. 8 in Greene & Lada 1996). Taking everything together, our NIR data strongly suggest that SVS 16 is a class II or class III YSO. Thus, the amount of circumstellar matter seems to be rather small.

However, these arguments derived from NIR data can constrain only the amount of hot or warm circumstellar matter relatively close to the stars. We can derive upper limits to the possible amount of cold circumstellar matter, i.e. material at distances of more than a few 100 AU from the stars, from the upper limits to the 350 μm and 1.3 mm fluxes given above. Using dust opacities appropriate for circumstellar matter around young stars (e.g. Preibisch et al. 1993; Ossenkopf & Henning 1994), these flux limits roughly transform into mass upper limits in the range $0.1 - 0.3\,M_\odot$. Thus, we cannot fully exclude the possibility that the SVS 16 binary might be surrounded by a circumbinary envelope or disk. However, we emphasize that there is no direct evidence for this possibility.

Our results suggest that SVS 16 has dissipated most of its circumstellar material very quickly, in less than a few 10^5 years. This dissipation time scale is very short, considering that many well studied classical T Tauri stars with large infrared excesses seem to be at least several 10^6 years old (e.g. Kenyon & Hartmann 1995). At the end of the next chapter we will consider a possible explanation for this.

6. ROSAT X-ray observations

We have obtained deep ROSAT pointed X-ray observations of the NGC 1333 star forming region with the HRI as well as with the PSPC detector. These data are described below. For details on the ROSAT satellite and its instruments, we refer to Trümper (1983), Pfeffermann et al. (1988), and David et al. (1996). We also investigated the data of the ROSAT All-Sky Survey. SVS 16 was not detected as an X-ray source in the survey, what is no surprise since the sensitivity of the survey data is about a factor of 20 less than that of our deep pointed observations. From the survey data we derive an upper limit for the PSPC count rate of < 0.036 cnts/sec.

6.1. HRI data

The 40 ksec deep HRI observation in which X-rays from SVS 16 were detected for the first time has be analyzed and discussed in detail by Preibisch (1997). Here, we just summarize the basic results: SVS 16 was clearly detected as an X-ray source with a background subtracted source count rate of 0.8 ± 0.2 cnts/ksec. A Kolmogorov-Smirnov Test suggested the count rate to be variable (probability of variability: 0.97), however, there seems to be only irregular variability not exceeding a factor of 2–3. Although we cannot study the X-ray variability very well because the count rate and thus the S/N of the light curve is very low, we can at least exclude a large X-ray flare like that observed on YLW 15 (Grosso et al. 1997) during our observation.

6.2. New ROSAT PSPC data

On 28 February and 1 March 1997, we performed a 8.9 ksec ROSAT PSPC pointed observation of SVS 16. In comparison with the HRI, the PSPC has higher sensitivity and spectral resolution, but much lower spatial resolution. In our PSPC image, 43 sources could be detected, among them all HRI sources with the exception of the faint HRI source X 6. In both the HRI and the new PSPC image, we find three sources within $90''$ of the IR position of SVS 16, namely HRI X10 = BD $+30°547$, X11 = SVS 16, and X13 = HJ 4 (see Fig. 7). In particular, SVS 16 itself is detected as a weak source in the PSPC image with a background subtracted count rate of 3.5 ± 1.2 cts/ksec. The number of detected photons is too small for a meaningful analysis of the X-ray spectrum. Nevertheless, we can get some spectral information from the ROSAT hardness ratios, which are defined by

$$HR1 = \frac{S_h + S_m - S_s}{S_h + S_m + S_s} \quad \text{and} \quad HR2 = \frac{S_h - S_m}{S_h + S_m}$$

with count rates $S_{s,m,h}$ in the soft ($0.1 - 0.4$ keV), medium ($0.5 - 0.9$ keV), and hard ($0.9 - 2.1$ keV) band, respectively. No source counts from SVS 16 could be detected in the soft band, yielding $HR1 = 1$ with a lower limit of $HR1 \geq 0.62$. This can easily be understood by the strong absorption of soft X-rays caused by the large extinction. For the second hardness ratio we find $HR2 = 0.14 \pm 0.25$.

We did not find any significant variations of the count rate. A Kolmogorov-Smirnov Test gave a probability of variability of only 0.42. We thus conclude to observe quiescent X-ray emission. Furthermore, the X-ray luminosity derived from the PSPC count rate agrees well with that derived from the HRI count rate (see below). This shows that the X-ray luminosity of SVS 16 during the PSPC observation was about the same as during the HRI observation, i.e. 2.5 years earlier.

6.3. X-ray luminosity

In order to compute the X-ray luminosity from the observed count rate, one has to specify the form of the X-ray spectrum. We interpret the X-ray emission as optically thin thermal plasma emission (see Raymond & Smith 1977). In the simplest model of isothermal emission, the X-ray spectrum can be described by the plasma temperature and the extinction. For the extinction we use $A_V = 26.2$ mag as found above, and the relation $N_{\rm H} = A_V \times 1.8 \times 10^{21}\,{\rm cm}^{-2}$ (Paresce 1984; see also Predehl & Schmitt 1995). The plasma temperature can in principle be determined by a fit to the X-ray spectrum, however for SVS 16 the number of detected source photons is too small for a detailed spectral analysis. We thus assume a plasma temperature of $kT = 1$ keV, which is typical for active stellar X-ray sources (cf. Schmitt et al. 1990) and also for T Tauri stars (e.g. Neuhäuser et al. 1995; Preibisch et al. 1996). Furthermore, this temperature is fully consistent with the observed spectral hardness: For an extinction of ~ 26 mag the hardness ratios given above suggest a Raymond Smith plasma temperature in the range $0.7-1.4$ keV (cf. Fig. 4 of Neuhäuser et al. 1995). We also note that in a recent deep ASCA observation of the NGC 1333 region, SVS 16 was detected only in the soft ASCA band ($0.5-2$ keV) but not in the hard band ($4-10$ keV) (Koyama, priv. comm.). We thus see no indication for a significantly higher or lower plasma temperature and believe that 1 keV should be appropriate.

With the parameters $N_{\rm H} = 4.7 \times 10^{22}\,{\rm cm}^{-2}$ and $kT = 1$ keV we computed a model X-ray spectrum and determined the transformation factor between count rate and *de*reddened X-ray flux by folding this spectrum through the detector response function with the corresponding EXSAS commands. We found that a PSPC count rate of 1 cnts/sec corresponds to a *de*reddened X-ray flux in the $0.1 - 2.4$ keV ROSAT band of $5.21 \times 10^{-9}\,{\rm erg/sec/cm}^2$. For the HRI, a count rate of 1 cnts/sec corresponds to $1.95 \times 10^{-8}\,{\rm erg/sec/cm}^2$. Since the computation of the transformation factor is a crucial step in the calculation of the X-ray luminosity, we performed an additional check and also computed these transformation factors with the Portable Interactive Multi-Mission Simulator (PIMMS), provided by the High Energy Astrophysics Science Archive Research Center. We found very good agreement of the EXSAS and PIMMS results.

With these transformation factors we derive an X-ray luminosity of $(1.8 \pm 0.5) \times 10^{32}$ erg/sec for the HRI data, and, in good agreement, $(2.0 \pm 0.7) \times 10^{32}$ erg/sec for the PSPC data. The fractional X-ray luminosity of SVS 16 [2] is $L_{\rm X}/L_{\rm bol} = 8 \times 10^{-3}$, and for the X-ray surface flux we find $F_{\rm X} = 1.1 \times 10^8\,{\rm erg/sec/cm}^2$. We note that the last two values are independent of the assumed distance and thus are valid even if we would have overestimated the distance to SVS 16. The X-ray luminosity of SVS 16 exceeds the solar value by nearly five orders of magnitude (cf. Table 4), its fractional X-ray luminosity is 10 000 times higher than that of the Sun. Finally, we note that the quoted X-ray luminosity includes only the flux in the $0.1 - 2.4$ keV band. If we extrapolate this to the flux in the total X-ray band ($0.1 - 100$ keV), the total X-ray luminosity is higher by a factor of about 4.8. This means that SVS 16 radiates as much as some 4% of its total luminosity in X-rays.

6.4. How to explain the extreme X-ray properties?

For a proper assessment of these results we now will compare the X-ray properties of SVS 16 to those of different classes of X-ray active stars. Since we could find no evidence for flares on SVS 16, we will consider only quiescent X-ray emission. We start with the class of T Tauri stars. These YSOs show X-ray luminosities exceeding the solar level by factors of 100 to 1000. Nevertheless, their X-ray properties can be explained by enhanced solar like coronal activity due to their fast stellar rotation (c.f. Montmerle et al. 1993). We have collected ROSAT X-ray data for all X-ray detected T Tauri stars in the star forming regions ρ Oph (Casanova et al. 1995), Chamaeleon I (Feigelson et al. 1993), IC 348 (Preibisch et al. 1996), NGC 1333 (Preibisch

[2] Since the two components of SVS 16 are not resolved in the X-ray data, we use the system luminosity and surface area to compute these values.

Table 4. The X-ray properties of SVS 16 compared to those of other classes of stellar X-ray sources. The references for the T Tauri stars are given in the text, RS CVn data are from Dempsey et al. (1993).

	quiet Sun	T Tauri stars median	T Tauri stars maximum	RS CVn maximum	SVS 16
$L_{\rm X}$ [erg/sec]	3×10^{27}	1×10^{30}	6×10^{31}	7×10^{31}	2×10^{32}
$L_{\rm X}/L_{\rm bol}$	8×10^{-7}	5×10^{-4}	3×10^{-3}	3×10^{-3}	8×10^{-3}
$F_{\rm X}$ [erg/sec/cm^2]	5×10^{4}	8×10^{6}	6×10^{7}	1.6×10^{8}	1.1×10^{8}

1997), Orion (Gagné et al. 1995), and Taurus (Neuhäuser et al. 1995). For more than 270 stars X-ray luminosities are known, for most of them also $L_X/L_{\rm bol}$, and for some of them also the X-ray surface fluxes. The median and maximum values of these three quantities are summarized in Table 4. The X-ray luminosity of SVS 16 exceeds that of any known T Tauri star by at least a factor of 3. SVS 16 also exceeds all reported $L_X/L_{\rm bol}$ ratios and X-ray surface fluxes for T Tauri stars.

Is it still possible to explain the extreme X-ray properties of SVS 16 as coronal activity? To investigate this question, we now will compare SVS 16 to the most coronally active stars, the RS CVn systems. These systems are close binaries, in which tidal forces cause very high stellar rotation rates, leading to extremely high levels of coronal activity. While SVS 16 seems to exceed any RS CVn in terms of absolute and fractional X-ray luminosity (see Table 4), there is at least one RS CVn system, BD$+25^\circ 580$, which shows an even higher X-ray surface flux than SVS 16. This means, that the extreme X-ray activity of SVS 16 can probably still be explained by coronal emission. While the separation of the two components in SVS 16 is far too large to produce tidal effects, one or both components might be RS CVn like systems.

Finally, we note that there seems to exist a class of YSOs, which are qualitatively similar to SVS 16 in the sense that they are very young, essentially free of circumstellar matter, and very strong X-ray sources: André et al. (1992) could detect a small population of class III YSOs with rather strong nonthermal radio emission in the ρ Oph star forming region. These objects seem to be younger than the majority of the T Tauri stars and thus must have cleared their circumstellar material very quickly. Their radio properties indicate that these objects have very extended magnetic structures, which might be explained by strong primordial magnetic fields. André et al. (1992) speculate that the conservation of the strong fossil magnetic fields might have caused the very fast dispersion of their circumstellar matter. Interestingly, these objects are among the X-ray brightest YOSs in the ρ Oph star forming region (Casanova et al. 1995). Thus, strong primordial magnetic fields might cause not only fast clearing of the circumstellar material, but also very high X-ray activity. Perhaps, SVS 16 is an extreme (the most X-ray luminous) example of such an object.

7. Summary and conclusions

We have shown that SVS 16 is a highly obscured young stellar object in the NGC 1333 star forming region. It is a binary system consisting of two very young (probably less than a few 10^5 yrs old) M-type PMS stars. In our observations we could not detect significant amounts of circumstellar matter associated with SVS 16. The high extinction is probably mainly caused by dust absorption in the molecular cloud material in front of SVS 16. Despite its youth, the system has already accreted or dispersed nearly all of its circumstellar material.

An extremely high, quiescent soft X-ray luminosity of 2×10^{32} erg/sec is confirmed by our new ROSAT data. This is the highest value ever found for the non-flaring X-ray emission from a late type star. An extrapolation to the total X-ray band shows that SVS 16 radiates about 4% of its energy as X-rays. These X-ray properties are extreme, but we believe that they can still be explained by coronal activity, since the X-ray surface flux we derive for SVS 16 does not exceed those of the most coronally active RS CVn binaries.

SVS 16 is in many aspects qualitatively similar to some very young and very X-ray active class III sources, which probably possess strong fossil magnetic fields. This, and the fact that coronal activity is assumed to be strongly linked to stellar rotation, offers an interesting explanation for the properties of SVS 16: The strong fossil magnetic field of the YSO caused a very quick clearing of the circumstellar matter. Due to the lack of a circumstellar disk, the magnetic coupling between the YSO and its disk, which is believed to brake the stellar rotation of YSOs (cf. Camenzind 1990; Königl 1991) could not work for SVS 16. Therefore, the stellar contraction caused a strong spin-up of the YSO and the rapid rotation might finally be the reason for its extreme X-ray activity.

Acknowledgements. Th. P. would like to thank G.H. Herbig and all other members of the Institute for Astronomy at the University of Hawaii in Honolulu for their hospitality during a prolonged stay in autumn 1997. Special thanks go to K.-W. Hodapp, J. Deane, and M. Nassir for useful discussions about SVS 16 and for providing us with an upper limit from their SHARC data before publication. We would like to thank the UKIRT staff for performing observations of SVS 16 as part of the service programme, and an anonymous referee, who's report helped to inprove this paper significantly.

This work was supported by the DFG under grants Yo 5/18-1,2, Ge 625/7-1,2, and Zi 242/9-1 in the "Physik der Sternentstehung" Program. The ROSAT project was supported by the Bundesministerium für Bildung, Wissenschaft, Forschung und Technologie (BMBF/DLR) and the Max-Planck-Society. The United Kingdom Infrared Telescope

is operated by the Joint Astronomy Centre on behalf of the U.K. Particle Physics and Astronomy Research Council. Some of the data have been collected at the European Southern Observatory, La Silla, Chile. This research has made use of data obtained through the Space Telescope European Coordinating Facility and the High Energy Astrophysics Science Archive Research Center (HEASARC), provided by NASA's Goddard Space Flight Center.

References

Adams F.C., Lada C.J., Shu F.H., 1987, ApJ 312, 788
André P., Montmerle T., 1994, ApJ 420, 837
André P., Deeney B.D., Phillips R.B., Lestrade J.-F., 1992, ApJ 401, 667
Aspin C., Sandell G., 1997, MNRAS 289, 1
Aspin C., Sandell G., Russel A.P.G., 1994, A&AS 106, 165
Bachiller R., Cernicharo J., 1986, A&A 166, 283
Bate M.R., Bonnell A., 1997, MNRAS 285, 33
Barsony M., Kenyon S.J. Lada E.A., Teuben P.J. 1997, ApJS 112, 109
Beichmann C.A., Soifer B.T., Helou G., et al., 1986, ApJ 308, L1
Brandner W., Zinnecker H., 1997, A&A 321, 220
Brinkmann W., Kawai N., Ogasaka Y., Siebert J., A&A 316, L9
Camenzind M., 1990, In: Klare G. (ed), Reviews in Modern Astrononmy 3, p. 234
Casanova S., Montmerle T., Feigelson E.D., André P., 1995, ApJ 439, 752
Cernis K., 1990, Astron. Space Sci. 166, 315
D'Antona F., Mazzitelli I., 1994, A&AS 90, 467
David L.P., Harnden F.R., Kearns K.E., Zombeck M.V., 1996, The ROSAT High Resolution Imager calibration report. SAO technical report
Dempsey R.C., Linsky J.L., Flemming T.A., Schmitt J.H.M.M, 1993, ApJS 86, 599
Feigelson E.D., Casanova S., Montmerle T., Guibert J., 1993, ApJ 416, 623
Gagné M., Caillault J.P., Stauffer J.R., 1995, ApJ 445, 280
Ghez A.M., White R.J., Simon M., 1997, ApJ 490, 353
Greene T.P., Lada C.J., 1996, AJ 112, 2184
Greene T.P., Lada C.J., 1997, AJ 114, 2157
Greene T.P., Meyer M.R., 1995, ApJ 450, 233
Greene T.P., Wilking B.A., André P., Young E.T., Lada C.J., 1994, ApJ 434, 614
Grosso N., Montmerle T., Feigelson E.D., et al., 1997, Nat, 387, 56
Hartigan P., Strom K.M., Strom S.E., 1994, ApJ 427, 961
Herbig G.H., 1998, ApJ 497, 736
Hünsch M., Schmitt J.H.M.M., Schröder K.-P., Reimers D., 1996, A&A 310, 801
Hunter T.R., Benford D.J., Serabyn E., 1996, PASP 108, 1024
Kamata Y., Koyama K., Tsuboi Y., Yamauchi, S., 1997, PASJ 49, 461
Kenyon S.J., Hartmann L., 1995, ApJS 101, 117
Käufl H.U., Jouan R., Lagage P.O., Masse P., Mastreau P., Tarrius A.: 1994, Infrared Phys. Technol. 35, No. 2/3, 203
Königl A., 1991, ApJ 370, L39
Koyama K., Hamaguchi K., Ueno S., Kobayashi N., Feigelson E.D., 1996, PASJ 48, L87
Lada C.J., 1987, In: Peimbert M., Jugaku J. (eds.), Star forming regions, IAU Symposium 115, Reidel, Dordrecht, p. 1
Lada E.A., Alves J., Lada C.J., 1996, AJ 111, 1964
Lefloch B., Castes A., Cernicharo J., Langer W.D., Zylka R., 1998, A&A 334, 269
Montmerle T., 1996, In: Pallavicini R., Dupree A.K. (eds.) 9th Cambridge Workshop on Cool Stars, Stellar System, and the Sun, ASP Conference Series Vol. 109, p. 405
Montmerle T., Feigelson E.D., Bouvier J., André P., 1993, In: Levy E.H., Lunine J.I. (eds.), Protostars and planets III, University of Arizona Press, p. 689
Neuhäuser R., Preibisch Th., 1997, A&A 322, L37
Neuhäuser R., Sterzik M.F., Schmitt J.H.M.M., Wichmann R. Krautter, J., 1995, A&A 297, 391
Ossenkopf V., Henning Th., 1994, A&A 291, 943
Palla F., Stahler S.W., 1990, ApJ 360, L47
Paresce F., 1984, AJ 89, 1022
Pfeffermann E., et al., 1988, In: Proc. SPIE 733, 519
Predehl P., Schmitt J.H.M.M., 1995, A&A 293, 889
Preibisch Th., 1997, A&A 324, 690
Preibisch Th., Ossenkopf V., Yorke H.W., Henning Th., 1993, A&A 279, 577
Preibisch Th., Zinnecker H., Herbig G.H., 1996, A&A 310, 456
Raymond J.C., Smith B.W., 1977, ApJS 35, 419
Rieke G.H., Lebofsky M.J., 1985, ApJ 288, 618
Roddier C., Roddier F., Northcott M.J., Graves E.J., Jim K., 1996, ApJ 463, 326
Ryter C., 1996, Astrophys. Space Science 236, 285
Sandell G., Knee L.B.G., Aspin C., Robson E.I., Russel A.P.G., 1994, A&A 285, L1
Schmitt J.H.M.M., Collura A., Sciortino S., Vaiana G.S., Harnden F.R., Rosner R., 1990, ApJ 365, 704
Siess L., Forestine M., Bertout C., 1997, A&A 326, 1001
Strom S.E., Grasdalen G.L., Strom K.M., 1974, ApJ 191, 111
Strom S.E., Vrba F., Strom K.M., 1976, AJ 81, 314
Trümper J., 1983, Adv. Space Res. 2, 241
Walter F.M., Brown A., Mathieu R.D., Myers P.C., 1988, AJ 96, 297
Ward-Thompson D., Buckley H.D., Greaves J.S., Holland W.S., André P., 1996, MNRAS 281, L53
Wilking B.A., McCaughrean M.J., Burton M.G., Giblin T., Rayner J.T., Zinnecker H., 1997, AJ 114, 2029
Zimmermann H.U., Belloni T., Izzo, C., Kahabka P., Schwentker O., 1993, EXSAS User's Guide, MPE Report 244, Garching